Supplemental material for 'Eliminating object prior-bias from sparse-projection tomographic reconstructions'

This supplementary material consists of details which we did not include in the main paper for purposes of brevity. This document consists of links to view our complete 3D reconstructions, an alternate simpler motivation for the use of multiple eigenspaces, and an alternate method to compute the parameters for the weights map. We also include a comparison with a method in literature based on comments from a reviewer.

Contents

1 Links to view our 3D reconstructions

Here we present the 3D reconstruction results discussed in Sec. 6 of the main paper. For each dataset, the links contain 2 videos: one showing all the templates and test volumes, and the other showing the reconstructed volumes by various methods. The videos are in `.avi` format and display reconstructions in a slice-by-slice manner.

- **Okra:**

  3D Okra of size $338 \times 338 \times 123$ was reconstructed from 45 cone-beam view measurements.

  https://www.dropbox.com/sh/vkol8aluzsnusfo/AABtu6-M1LKOsQjKIjxlSxUfa?dl=0

- **Potato:**

  3D Potato of size $150 \times 150 \times 100$ was reconstructed from 18 cone-beam view measurements.

  https://www.dropbox.com/sh/w16j7pvud2lbrpx/AACCJLxgoAurT2vVKIdu-MwFa?dl=0

- **Sprouts:**

  3D Sprouts of size $130 \times 130 \times 130$ was reconstructed from 30 cone-beam view measurements.

  https://www.dropbox.com/sh/y6s4h2p04tp1lgq/AADn2q43o7SYj10rmheMCDzZa?dl=0

2 Using multiple eigenspaces

Here we present a schematic explaining the advantage of using multiple eigenspaces within the proposed spatially-varying reconstruction technique. This may be viewed as a simpler version of the somewhat long algorithm described in the main paper.

Schematic 1: Motivation behind our algorithm. (The plus $\oplus$ and the minus $\ominus$ operators are placeholders; precise details available in Section 5 of the main paper).
Let prior $Q :=$ old regions (O)
Let test volume $\boldsymbol{x} :=$ old regions $(O) \oplus$ new regions (N)

1. Compute pilot reconstruction of $\boldsymbol{x}$. Let this be called X.
   $X = O \oplus N \oplus Ar(O) \oplus Ar(N)$, where
   $Ar(O)$ denote the reconstruction artefacts that depend on the old regions, the imaging geometry and the reconstruction method, and
   $Ar(N)$ denote the reconstruction artefacts that depend on the new regions, imaging geometry and the reconstruction method.
2. Note that $Q \ominus X = N \oplus Ar(O) \oplus Ar(N)$ gives the new regions, but along with lots of artefacts due to the imaging geometry (sparse views). To eliminate these unwanted artefacts, compute $Y = Q \oplus Ar(O)$ by simulating projections from Q using the same imaging geometry used to scan $\boldsymbol{x}$, and then reconstructing a lower quality prior volume Y.
3. Note that $Y \ominus X = N \oplus Ar(N)$ contains the artefacts due to the new regions only. These are different for different reconstruction methods. To eliminate these method dependent artefacts, compute Y and X using different reconstruction methods. Let these be denoted by Y^j and X^j respectively.
4. Compute
   $$Y^1 \ominus X^1 = N \oplus Ar^1(N)$$
   $$Y^2 \ominus X^2 = N \oplus Ar^2(N)$$
5. New regions are obtained by computing
   $$(Y^1 \ominus X^1) \cap (Y^2 \ominus X^2) = N$$
6. Finally, assign space-varying weights $\boldsymbol{W}$ based on step 5.

3 Learning-based computation of weights map

The value of k (discussed in Sec. 7 of the main paper) is typically dependent on the number of false positives the system can allow in exchange for the detection of more true positives (regions of new changes). It is this choice and not the particular type of dataset that affects the selection of k. In our work, the chosen k corresponds to the one that gives minimal tolerance to false positives. However, in case one wishes to completely avoid the use of this hyper-parameter, one can construct a binary weights-map using a method described below.

1. For the purposes of training, treat one of the previously scanned images as test. Annotate the region of differences between the test and all of the previously scanned images based on domain knowledge.
2. Compute the difference between the pilot reconstruction of the test and its projection onto the eigenspace. Let this spatial map be called 'error map'.
3. Train a Support Vector Machine (SVM) model (or any other classifier model) to classify patches of this error-map image into one of the two categories: new changes present, new

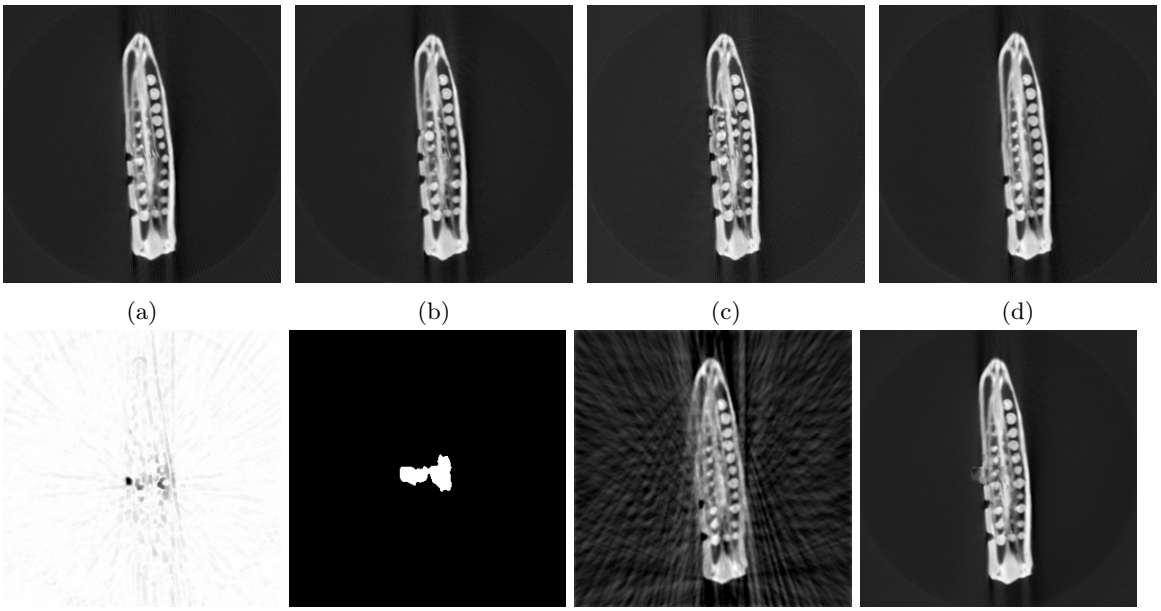

Figure 1: Using an alternate approach to generate (binary) weights map. (a)-(c) the images used as object-prior, (d) the test (310×310). Measurements along 60 views were taken. (e) error-map showing new regions, (f) detected binary weights map showing regions of new changes, (g) pilot, (h) final reconstruction with pilot in the new regions, and prior in the other regions.

changes absent.

4. Once the trained SVM model is obtained, apply the model and generate binary weights-map for new test images in the same longitudinal study.

5. Once the binary weights-map $\boldsymbol{W_b}$ is obtained, use these in the alternate minimization optimization described in Eq. 7 of the main paper.

We mention in passing that if we are to entirely avoid the other parameters (viz. λ_1 and λ_2, the prior and the pilot can be stitched in a simplistic way using the equation $\boldsymbol{W_b}$(Pilot)+(1−$\boldsymbol{W_b}$)(Prior). The advantage of this method is that the computational time is signficantly reduced since the alternate minimization procedure is not used.

4 Empirical comparison with a method in literature: Detecting new changes directly in the measurements

Sec. 2 of the main paper ('Related work') contrasts the spatially-varying technique with other prior based techniques in literature. Here we present a 2D reconstruction result (of the test shown in Figure. 2) to compare our method with [1], in which the new changes are directly detected in the measurement space by computing the difference between the measurements of the test and the corresponding simulated measurements of the template. This difference-volume is then reconstructed

and then fused (added to) with the original high quality template. However, in the above method, the sub-sampling artefacts present in the difference-volume gets carried over to the final reconstructed image. This is shown in Figure 3. A quantitative comparison over the region of interest is shown in Table 1.

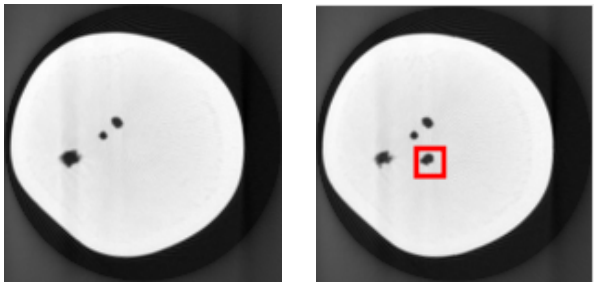

(a) Template (b) Test

Figure 2: Template and test from the Potato dataset for the reconstructions shown in Figure. 3

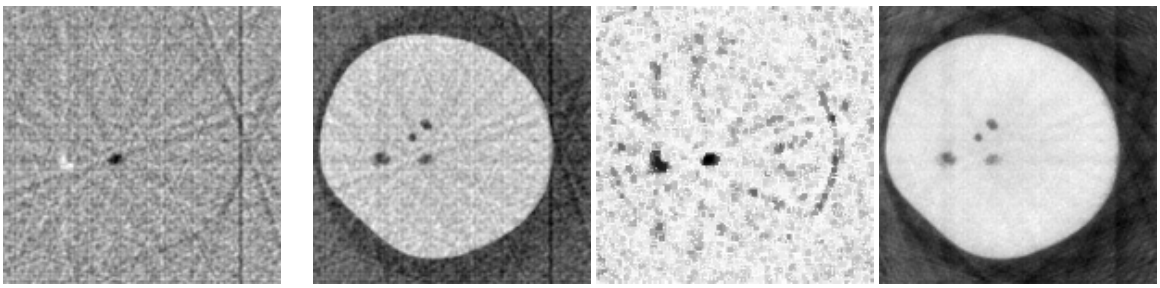

(a) [1]:new-changes (b) [1]:Reconstruction (c) Our weights-map (d) Our reconstruction

Figure 3: Reconstruction of the test in Figure 2. Reconstructions were performed from 12 views. Gaussian noise of 0 mean and SD = 1% of mean of measurements, was added to the measurements.

Table 1: SSIM values (within RoI) of reconstructions shown in Figure 3.

	SSIM (whole image)	**SSIM (RoI)**
Method in [1]	0.65	0.60
This paper	0.89	0.92

References

[1] J. Lee, J. W. Stayman, Y. Otake, S. Schafer, W. Zbijewski, A. J. Khanna, J. L. Prince, and J. H. Siewerdsen, "Volume-of-change cone-beam CT for image-guided surgery," pp. 4969–89, Aug 2012.